PROCEEDINGS OF SCIENCE

Amorphous Carbon-coated Storage Cell Tests for the Polarized Gas Target at LHCb

R. Engels,[a,b,*] **P. Costa Pinto,**[c] **P. Di Nezza,**[d] **T. El-Kordy,**[e,b] **M. Ferro-Luzzi,**[c] **K. Grigoryev,**[a] **C. Kannis**[f] **and S. Pütz**[g,a]

[a] *GSI, Helmholtzzentrum für Schwerionenforschung, Planckstraße 1, Darmstadt, Germany*
[b] *Institut für Kernphysik, Forschungszentrum Jülich, Wilhelm-Johnen-Straße 1, Jülich, Germany*
[c] *European Organization for Nuclear Research, CERN, Esplanade des Particules 1, Geneva, Switzerland*
[d] *Instituto Nazionale di Fisica Nucleare, Laboratori Nazionali di Frascati, Via Enrico Fermi 54, Frascati, Italy*
[e] *FH Aachen – University of Applied Sciences, Bayernallee 11, Aachen, Germany*
[f] *Institute for Laser and Plasma Physics, Heinrich-Heine-Universität Düsseldorf, Universitätsstraße 1, Düsseldorf, Germany*
[g] *Institute for Nuclear Physics, Universität zu Köln, Zülpicher Str. 77, Köln, Germany*

E-mail: r.w.engels@fz-juelich.de

The LHC beams cannot be polarized. Hence, the implementation of a dense polarized gas target at the LHCb experiment at CERN, to be operated simultaneously with beam-beam collisions, will enable fixed target interactions to explore a new energy range of spin physics measurements. Unfortunately, typical surface coatings like water, Teflon or aluminium, normally used to avoid polarization losses, are forbidden due to vacuum and beam policies.

Using the former ANKE atomic beam source at Forschungszentrum Jülich to provide a polarized atomic hydrogen beam, we investigated the properties of a storage cell coated with amorphous carbon. A notable recombination rate, lying between 93 and 100%, and a preservation of polarization during recombination exceeding 74% was observed. We were able to generate H_2 molecules with a nuclear polarization of P∼0.59. Remarkably, no water layer accumulated on the cooled storage cell surface, even over extended periods. Furthermore, we examined the influence of Lyman-radiation on the recombination rate on carbon, addressing a prominent question in the field of astrophysics.

A similar talk was given at "1st Workshop on Polarized Beam and Target - Physics and Applications (PBT2024)" from 26.-28.02.2024 in Huizhou, China, by T. El-Kordy and is based on a corresponding paper [1].

20th International Workshop on Polarized Sources, Targets, and Polarimetry (PSTP2024)
22-27 September, 2024
Jefferson Lab, Newport News, VA

*Speaker

PoS(PSTP2024)050

1. Introduction

For the investigation of the spin dependence of the nuclear forces, polarized beams and targets are an inevitable tool in nuclear physics. Due to the fact that in storage rings the usable target density is limited to $\sim 10^{14}$ atoms/cm^2, storage cells are in common use to store polarized hydrogen or deuterium atoms of a polarized atomic beam source (ABS) [2–6]. The atomic jet from such a source [7] delivers up to 10^{17} atoms/s at velocities below 1000 m/s and, thus a target density below 10^{12} atoms/cm^2. A key advantage of these jet targets is their small beam-target interaction volume, which can, in some cases, supersede the importance of high statistics [8]. In fact, collecting these atoms in T-shaped storage cells significantly increases luminosity by two orders of magnitude, with a compromise often acceptable for many experiments. The only price to pay due to the longer interaction volume, up to 40 cm long cells have been used, is acceptable for many experiments.
Nevertheless, the surface coating of such cells is a critical aspect, because the hydrogen atom itself is a chemical radical. Therefore, it is able to react with many materials, leading to a loss of nuclear polarization. Over the years, a few materials have been found that helps to avoid the recombination of the atoms into molecules, which is the dominant process. Besides a Teflon coating, aluminum cells [7] allow to avoid the recombination process and preserve the polarization of the atoms to a high degree. If the cell is cooled to further increase the target density by reducing the velocity of the atoms inside, the built-up of a thin water film was observed. This water-ice coated surface is the best material to avoid the recombination process and the corresponding polarization losses so far [9]. Several other materials known to be inert enough to avoid the recombination were not helpful as storage cell coatings.
Further investigations of these processes at different accelerators have shown that during the recombination process nuclear polarization can survive at least partially. It was found that non-magnetic metal surfaces like gold or copper limits the nuclear polarization in the molecules by 50% of the atomic polarization [10, 11]. Other materials showed similar results [12]. This could be explained by the Eley-Rideal mechanism: One hydrogen atom is bound on the surface and loses its nuclear polarization more or less immediately due to magnetic field gradients induced by free electrons in the metals. Then, this atom can recombine on the surface with a second, still polarized atom from the gas phase. By that, only the spin of the second atom is preserved and the polarization of the molecules does not exceed 50% of the atomic polarization.
With the ABS of the ANKE experiment at COSY/Jülich, normally utilized to feed such a storage cell with polarized atoms to serve as polarized internal target, more detailed investigations are made without using the accelerator (see Fig. 1). The corresponding measurements of the recombination rate and polarization verified the former results [13], and furthermore, a different recombination mechanism was observed on Fomblin oil that shows a nearly full polarization preservation in the molecules. Running the ABS with hydrogen and deuterium in parallel enabled the production of HD molecules with dedicated nuclear spins for the protons and deuterons respectively [14].
In the coming years, it is foreseen to implement such a polarized internal target in front of the LHCb detector at CERN [15] to investigate polarized collisions at high energies. However, the beam and vacuum policies at CERN do not allow the usage of the conventional surface coatings like aluminum (secondary-electron yield too high), Teflon (insulator), or water (vacuum problems!). Instead, amorphous carbon was proposed due to the fact that the relatively strong C-H bond should

be inert when attacked by atomic hydrogen.
Nevertheless, the absence of magnetic fields due to free electrons or nuclear spins gives some hope that the polarization lifetime of the incoming hydrogen atoms might be long enough to get polarized molecules. Therefore, further investigations are needed before this kind of surface coating can be used for a polarized internal storage-cell target along the LHC at CERN.
In astrophysics, it was proposed that in hydrogen clouds in the interstellar medium carbon dust might be a catalyst for the recombination of hydrogen atoms into molecules [16, 17] since a direct recombination is forbidden due to energy and momentum conservation. Nevertheless, actual investigations showed that most recombination mechanisms are not effective on carbon surfaces. Only a radiation-induced version of the Langmuir-Hinshelwood mechanism, where both atoms are bound on the surface before recombination, showed a reasonable cross section [18]. Thus, an external radiation source, e.g., a nearby star, is needed to break the C-H bond before recombination into H_2 is possible.

2. The Experimental Setup

The necessary experimental setup at the Institute for Nuclear Physics at Forschungszentrum Jülich (FZJ), as shown in Fig. 1, was built in a collaboration with the University of Cologne and the Petersburg Nuclear Physics Institute (PNPI). The ANKE ABS is feeding a T-shaped storage cell inside a superconducting solenoid cooled with liquid helium. The exchangeable storage cells are made from fused quartz with a thin gold layer, which can be coated with other materials in different ways, e.g. by sputtering, evaporating or galvanic methods. The polarized hydrogen/deuterium atoms in different hyperfine substates are sent into these cells where the atoms can recombine into molecules. An electron beam, originating from an electron gun on the left, is accelerated into the cell at a beam energy of about 100 eV, corresponding to the maximum of the ionization cross section. A positive potential along the cell induced by a voltage of a few kV at the gold layer will accelerate the ions into the Lamb-shift polarimeter (LSP) [19, 20] on the right. Here, the incoming ions recombine by charge exchange with Cesium vapor into metastable hydrogen atoms before their individual hyperfine substates are separated inside the spin filter. The residual metastable atoms that will have different nuclear spins at corresponding magnetic fields in the spin filter are quenched into the ground state and the induced Lyman-α (L_α) photons are registered with a photomultiplier. In addition, a Wien filter is able to separate the protons and the molecular ions so that the ion beam intensities and the polarization can be measured independently. Further details can be found in [13, 14].
The only possible photon source for a radiation-induced recombination process is the plasma of the ABS dissociator that is shining in bright magenta. This color stems from Balmer transitions of the atoms in the plasma, i.e. from transitions into the $n = 2$ state. But these photons do not have enough energy to break the C-H bond of 4.3 eV. Of course, Lyman transitions into the ground state with $n = 1$ at photon energies above 10.2 eV (L_α-transition from $n = 2$ into $n = 1$) will also occur, but most are not registered outside the plasma tube, because these photons are absorbed by the cooled glass walls of the dissociator. Nevertheless, some of these photons can leave the plasma through the nozzle along the beam axis of the ABS and reach the storage cell. To proof specifically the

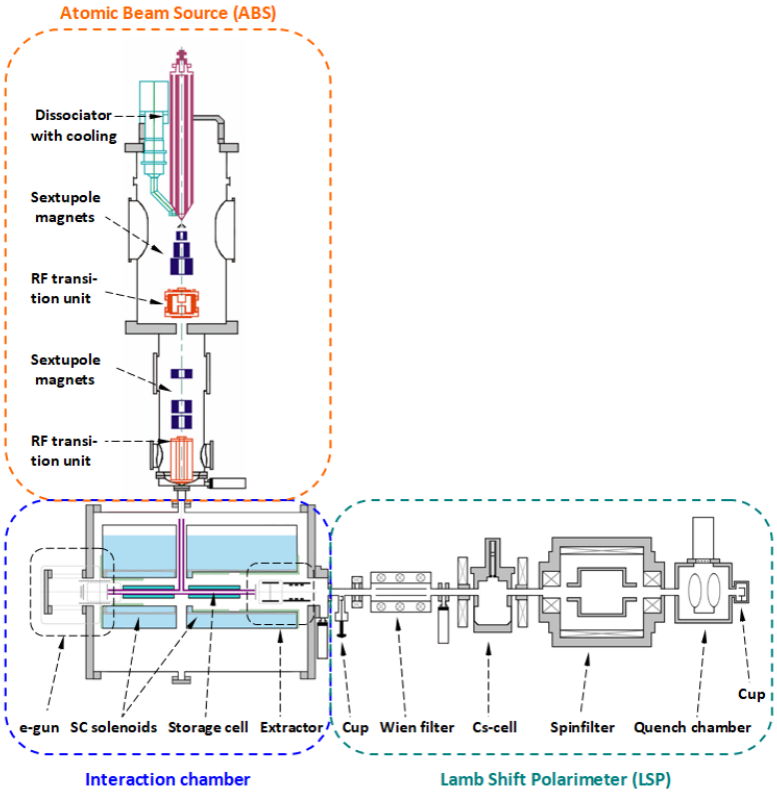

Figure 1: The design of the apparatus used to produce polarized molecules and measure their polarization. The ANKE ABS is feeding a storage cell with polarized atoms that can recombine on the cell coating. An electron beam from the left side ionizes atoms and molecules and the produced ions, i.e. protons, H_2^+ or H_3^+, are accelerated into a Lamb-shift polarimeter to determine the nuclear polarization.

L_α-radiation from the ABS, a small modification of the apparatus was made (see Fig. 2):
An aluminum rod that fits into the storage cell was cut by 45° and polished to reflect these L_α-photons onto the ion beam line of the LSP. In the last component of the LSP another aluminum mirror deflects these photons into the photomultiplier where they can be registered.

3. Results

Despite significant photon losses due to the long beam line and poor reflection of the aluminum mirrors, a clear signal was observed by the multiplier when the valve between the ABS chamber and the storage cell was opened. A naive estimation, based on the necessary cooling power for the dissociator of about 300 W and the assumption that at least 10% of the heating stems from absorbed L_α-photons, predicts that at least 10^{18} of these photons reach the storage cell per second, i.e. more than the number of hydrogen atoms.

With the Wien filter of the LSP, the accelerated ions leaving the cell can be separated, and their intensity measured with the Farraday cup at the end of the beam line. For this purpose, electric

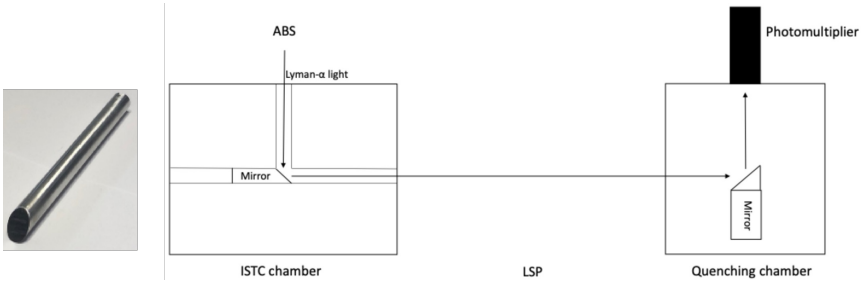

Figure 2: The setup of the Lyman-α measurements: The corresponding photons coming from the ABS are deflected by an aluminum mirror in the storage cell along the ion beam axis into the quenching chamber where they are reflected into the photomultiplier.

potentials are fixed and the magnetic field of the Wien filter is increased linearly in time (see Fig. 3). The ion beam intensity (yellow), the ramp signal proportional to the magnetic field (purple), and the photomultiplier signal (blue) were measured as a function of time. Which ion signal in the cup is

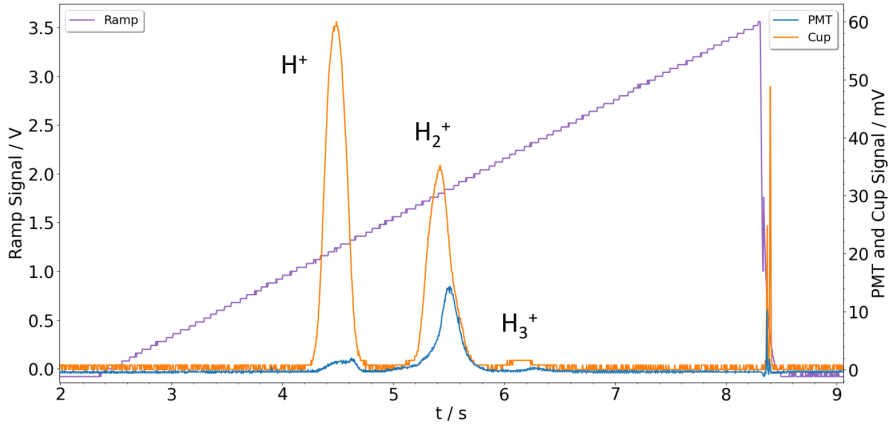

Figure 3: The ion beam intensity registered at the Faraday cup (yellow) and the photomultiplier (blue) when the magnetic field of the Wien filter is linearly increased (purple). Due to the different focusing, the proton signal in the cup is dominant, but with the photomultiplier more photons are measured when the molecular H_2^+ ions enter the quenching chamber.

dominant depends on the focusing of the ions, which is different for each type of ion because of the necessary mix of electric and magnetic fields in the individual components. The large proton intensity seen in the spectra of Fig. 3 hints at a low recombination rate, especially when it is considered that the ionization cross section for molecules into molecular ions is larger than for hydrogen atoms into protons. Even a considerable amount of protons is produced when H_2 molecules are ionized. Nevertheless, the presence of H_3^+ ions that are produced due to the reaction $H_2 + H_2^+ \rightarrow H_3^+ + H$ is a proof for a reasonable amount of molecules in the cell. Of course, the presence of the H_2^+ ions clearly indicates that recombination occurs inside the cell.

In parallel, the incoming ions are producing photons in the visible range of the photomultiplier between 110 and 165 nm. Again, the amplitudes of these peaks are not linearly correlated with the

beam intensities, because the cross sections for the production of the possible transitions to induce the respective photon energies are different.
In the next step, the Wien filter separates the H^+ and H_2^+ ions so that their nuclear polarization can be measured as a function of the magnetic field along the storage cell. Typical examples are found in Fig. 4. The signal intensity in the photomultiplier for both ions is very different, because

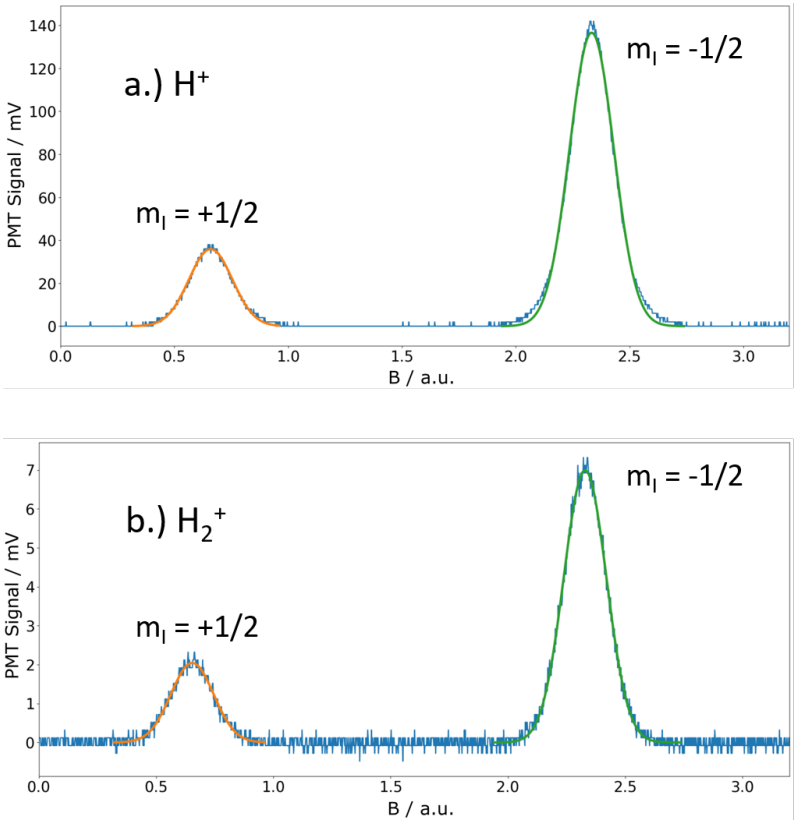

Figure 4: The measured Lyman-α spectra for H^+ (a) and H_2^+ (b) ions reaching the LSP. The magnetic field along the storage cell was set to 0.5 T and the observed nuclear polarization was $P_{H^+} = -0.584 \pm 0.002$ (a) for the protons and $P_{H_2^+} = -0.54 \pm 0.01$ (b) for the molecular H_2^+ ions.

the cross section to produce metastable hydrogen atoms, necessary for the spin separation in the spin filter differs by a factor of 35 ± 5. Thus, the signal for the proton beam is much stronger, with correspondingly lower statistical uncertainty compared to the molecular ions. Nevertheless, the measured polarization for both ions as a function of the magnetic field in the spin filter is very similar, as shown for protons in the example in Fig. 5. When hydrogen atoms in the 'pure' hyperfine substate 3 ($F = 1$ / $m_F = -1$ or m_J = -1/2 / m_I = -1/2) are sent into the storage cell, their nuclear polarization does not depend on the external magnetic field. Thus, if these atoms are ionized, the protons will have the same polarization as the original atom. Of course, when the atoms recombine into molecules, the nuclear polarization can change due to various recombination processes. But the nuclear polarization of the molecules in the cell depends on the external magnetic field, because the rotational magnetic moment of the molecule itself can now couple with the nuclear spins. Due to the fact that a hydrogen molecule is a system of fermions and, therefore, the total wave function must

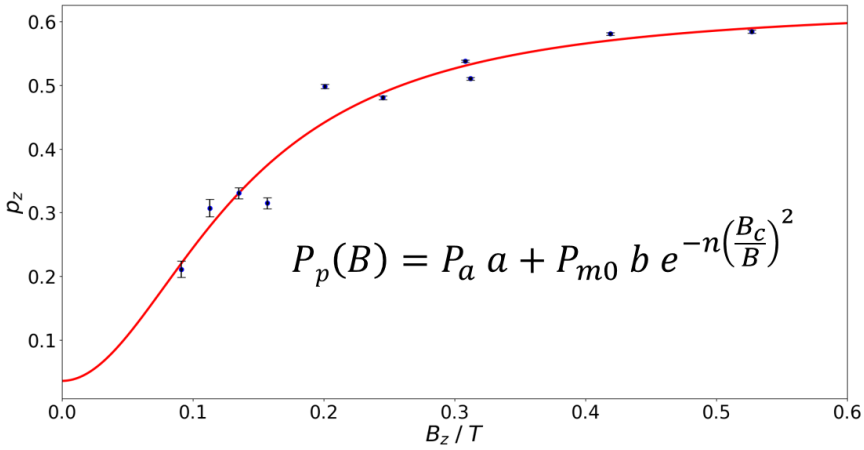

Figure 5: A fit of the measured proton polarization $P_p(n, B)$ as function of the external magnetic field B allows deducing the molecular polarization directly after recombination P_{m0}, the amount of wall collisions n, and the recombination rate.

be anti-symmetric, the rotational magnetic moment J must be odd when the spins of the protons are parallel (ortho-hydrogen). At the low temperatures of the storage cell, which can be varied between 40 and 120 K, the corresponding rotational magnetic moment will be mostly J=1. Thus, the coupling between J and the nuclear spins corresponds to a critical magnetic field B_c = 5.4 mT, about one order smaller than the coupling between the electron and nuclear spin in the ground state hydrogen atom. Now, every wall collision of the molecules is able to change m_J, which will immediately change m_I and, therefore, polarization might be lost. To avoid this polarization loss, the nuclear spins can be coupled to an external magnetic field $B >> B_c$ that is able to overcome the coupling to the rotational magnetic moment. Following ref. [11, 13], after n wall collisions inside the cell with a magnetic holding field B, the polarization of the molecule will be

$$P_m(n, B) = P_{m0} \cdot e^{-n(B_c/B)^2} \quad , \tag{1}$$

with P_{m0} as the nuclear polarization of the molecule directly after the recombination process. Thus, a measurement of the molecular polarization as function of the external magnetic field B allows for determining the average amount of wall collisions n in the cell and the original molecular polarization P_{m0}. Here, n depends on the geometry of the cell and the interaction of the molecules with the wall itself. For example, elastic scattering will provide a smaller n than absorption of the molecules on the surface before they leave again with a $\cos\theta$ or even $(\cos\theta)^2$ distribution.
Now, the protons in the ion beam stem either with probability a from hydrogen atoms or with probability b from molecules so that $a + b = 1$. As long as the polarization of atoms P_a in the pure states does not depend on the external field, the proton polarization will be:

$$P_p(n, B) = P_a \cdot a + P_{m0} \cdot b \cdot e^{-n(B_c/B)^2} \quad . \tag{2}$$

Therefore, a fit of this function to the measurement of the proton polarization additionally provides the parameters a and b, allowing for the determination of the recombination rate on the cell surface.

4. Conclusion

The measurement shown in Fig. 5 yields a molecular polarization $P_{m0} = -0.57 \pm 0.03$, an average amount of wall collisions of $n = 435 \pm 236$ and a recombination rate between 0.95 and 1. Thus, about 73% of the original atomic polarization P_a = -0.78 survived during the recombination process. The number of wall collisions is relatively large and might be attributed to the rough surface structure of the amorphous carbon or to absorption of the molecules on the surface before they leave in a $\cos\theta$ distribution.

Investigations from astrophysics show that the conventional recombination mechanism of hydrogen atoms into molecules does not work on an amorphous carbon surface [16]. In our case, the substantial amount of L_α photons from the dissociator and the following radiation-induced recombination explains the large recombination rate observed in these measurements. Thus, these L_α photons may also explain why other materials like Drifilm, which are known in chemistry for their low recombination rates, showed the opposite effect when used as storage cell coatings. In addition, this effect might be the reason why common surface coatings, i.e. aluminum, Teflon and water, are useful materials. At least for aluminum, it is known that it is the best reflecting material for the L_α wavelength of 121 nm. For water ice and Teflon, no known reflection efficiencies at this wavelength exists, but at slightly longer wavelength above 200 nm some transmission and reflection coefficients are known and hint at a suppression of this radiation-induced recombination mechanism.

5. Acknowledgments

C. Kannis acknowledges funding from the Deutsche Forschungsgemeinschaft (DFG, German Research Foundation) – 533904660.

References

[1] T. El-Kordy et al.; Nucl. Instrum. Meth. A **1068**, 169707 (2024).
DOI: 10.1016/j.nima.2024.169707

[2] E. Steffens and W. Haeberli; Rep. Prog. Phys. **66**, R02 (2003).
DOI 10.1088/0034-4885/66/11/R02

[3] K. Grigoryev et al.; Int. J. Mod. Phys. E **18**, 511 (2009).
DOI: 10.1142/S0218301309012574

[4] T. Wise et al.; Nucl. Instrum. Meth. A **336**, 410 (1993).
DOI: 10.1016/0168-9002(93)91252-I

[5] P. Lenisa et al.; Nucl. Instrum. Meth. A **536**, 244 (2005).
DOI: 10.1016/j.nima.2004.08.079

[6] M.V. Dyug et al.; Nucl. Instrum. Meth. A **495**, 8 (2002).
DOI: 10.1142/9789812777683_0010

[7] M. Mikirtytchiants et al.; Nucl. Instrum. Meth. A **721**, 83 (2013).
DOI: 10.1016/j.nima.2013.03.043

[8] A. Zelenski et al.; Nucl. Instrum. Meth. A **536**, 248 (2005).
DOI: 10.1016/j.nima.2004.08.080

[9] Chr. Baumgarten et al.; Nucl. Instrum. Meth. A **496**, 263 (2003).
DOI: 10.1016/S0168-9002(02)01750-3

[10] J.F.J. van den Brand et al.; Phys. Rev. Lett. **78**, 1235 (1997).
DOI: 10.1103/PhysRevLett.78.1235

[11] T. Wise et al.; Phys. Rev. Lett. **87**, 042701 (2001).
DOI: 10.1103/PhysRevLett.87.042701

[12] P. Lenisa et al.; AIP Conf. Proc. **675**, 939 (2003).
DOI:10.1063/1.1607273

[13] R. Engels et al.; Phys. Rev. Lett. **115**, 113007 (2015).
DOI: 10.1103/PhysRevLett.115.113007

[14] R. Engels et al.; Phys. Rev. Lett. **124**, 113003 (2020).
DOI: 10.1103/PhysRevLett.124.113003

[15] P. Lenisa et al.; contribution to this proceedings.

[16] S. Cazaux and A.G.G.M. Tielens; Astrophys. J. **575**, 29 (2002).
DOI: 10.1086/342607

[17] V. Wakelam et al.; Mol. Astrophys. **9**, 1 (2017).
DOI: 10.1016/j.molap.2017.11.001

[18] I. Alata, G.A. Cruz-Diaz, G.M. Muñoz Caro and E. Dartois; Astron. Astrophys. **569**, A119 (2014).
DOI: 10.1051/0004-6361/201323118

[19] R. Engels et al.; Rev. Sci. Instrum. **74**, 4607 (2003).
DOI: 10.1063/1.1619550

[20] R. Engels et al.; Rev. Sci. Instrum. **76**, 053305 (2005).
DOI: 10.1063/1.1898923